8416 *J. Am. Chem. Soc.* **1995,** *117,* 8416–8421

Theoretical Study of the Ionization of the H_2S-H_2S, PH_3-H_2S, and $ClH-H_2S$ Hydrogen Bonded Molecules

Mariona Sodupe, Antonio Oliva, and Juan Bertran*

Contribution from the Department de Química, Universitat Autònoma de Barcelona, Bellaterra 08193, Barcelona, Spain

Received February 13, 1995[®]

Abstract: Ab initio calculations that include correlation energy have been performed to study the first two vertical ionic states of H_2S-H_2S, PH_3-H_2S, and $FH-H_2S$ hydrogen bonded molecules and the subsequent rearrangement processes. In all cases, the first two ionic states are the $^2A'$ and $^2A''$ states depending on whether the ionization is located in the proton acceptor or in the proton donor, respectively. If ionization is produced in the proton donor monomer, the dimer evolves to a proton transfer complex, while if ionization is produced in the proton acceptor the dimer dissociates and then evolves to a three-electron hemibond complex. This hemibond structure is found to be the most stable isomer for all the systems. The obtained results are compared with those obtained from comparable calculations performed previously for the first-row H_2O-H_2O, NH_3-H_2O, and $FH-H_2O$ hydrogen bonded molecules.

Introduction

The study of the reactivity of clusters upon ionization is currently a very active area of research.[1] Removing an electron from the cluster changes the properties of the system completely leading to a very rich and varied chemistry. The generated radical cations can evolve via different chemical reactions such as electron transfer, proton transfer, or molecular rearrangements.

We have recently reported a study of the ionization of the first-row H_2O-H_2O, NH_3-H_2O, and $FH-H_2O$ hydrogen bonded molecules.[2] In this study we found that the two lowest ionic states arise from ionizing the proton donor monomer or the proton acceptor molecule. In the first case, there is an increase of the acidity of the proton donor molecule, which leads the dimer to evolve to a proton transfer complex. In the second case, the increase of acidity is produced in the proton acceptor monomer and because of that the dimer rearranges in such a way that the originally acceptor monomer acts as a proton donor in the final cation complex.

Although for the water−water and water−ammonia dimers the calculations at a correlated level showed that this ionic state could also evolve to three-electron hemibond complexes, none of these structures were found to be the global minimum of the potential energy surface. However, a systematic study of the first- and second-row symmetrical $(AH_n)_2{}^+$ cation dimers by Radom et al.[3] showed that for the second-row systems the singly charged three-electron hemibond complexes are more stable than their hydrogen bonded isomers. Thus, a different behavior might be expected between first-row and second-row hydrogen bonded complexes after ionization.

A few theoretical studies have been performed for the ionization of the $(H_2S)_2$ dimer.[4−6] They present some discrepancies in the nature of the relaxed radical cation and in the evolution of the second ionic state. That is, while Hartree−Fock (HF) calculations predict the proton-transfer complex, H_3S^+-SH, to be a stable minimum,[4,6] calculations at a correlated level find this isomer to collapse spontaneously to the hemibonded structure.[3] Moreover, the HF geometrical optimization of the second ionic state does not yield to a stable minimum but to the dissociation into the H_2S and H_2S^+ molecules.[6] This is in contrast to the $(H_2O)_2$ dimer for which calculations at a correlated level[2] showed that the relaxation of the second ionic state led to a three-electron hemibond structure. Calculations on the $(PH_3-H_2S)^+$ [7] and $(ClH-H_2S)^+$ [8] radical cations have been performed by Clark within the context of three-electron hemibond structures.[9,10] We are not aware of any theoretical study of the ionization and subsequent rearrangements of the PH_3-H_2S and $ClH-H_2S$ hydrogen bonded dimers.

In this paper we extend our previous study on the ionization of first-row hydrogen bonded molecules to the second-row analogs: H_2S-H_2S, PH_3-H_2S, and $ClH-H_2S$. This study will allow us to discuss the trends in this row and to contrast the nature of the ionic states and its role on the geometrical relaxation with those of the first-row hydrogen bonded dimers.

Methods

The level of theory used in the present work is the same as the one used in our previous study on the ionization of first-row hydrogen bonded molecules.[2] That is, because inclusion of correlation energy was shown to be necessary to obtain three-electron hemibond structures in the geometry relaxation of the ionized hydrogen bonded dimer, the geometry optimizations and frequency calculations are performed including electron correlation at the MP2 level.[11] Single-point calculations using the size extensive modified-coupled-pair functional MCPF

[®] Abstract published in *Advance ACS Abstracts,* July 1, 1995.

(1) Brutschy, B. *Chem. Rev.* **1992**, *92*, 1567.

(2) Sodupe, M.; Oliva, A.; Bertran, J. *J. Am. Chem. Soc.* **1994**, *116*, 8249.

(3) Gill, P. M. W.; Radom, L. *J. Am. Chem. Soc.* **1988**, *110*, 4931.

(4) Fernández, P. F.; Ortiz, J. V.; Walters, E. A. *J. Chem. Phys.* **1986**, *84*, 1653.

(5) Ortiz, J. V. *Chem. Phys. Lett.* **1987**, *134*, 366.

(6) Pradeep, T.; Rao, C. N. R. *Chem. Phys. Lett.* **1991**, *185*, 496.

(7) Clark, T. *J. Comp. Chem.* **1983**, *4*, 404.

(8) Clark, T. *J. Comp. Chem.* **1982**, *3*, 112.

(9) Clark, T. *J. Comp. Chem.* **1981**, *2*, 261.

(10) Clark, T. *J. Am. Chem. Soc.* **1988**, *110*, 1672.

(11) Krishnan, R.; Pople, J. A. *Int. J. Quantum Chem.* **1978**, *14*, 91.

(12) Chong, D. P.; Langhoff, S. R. *J. Chem. Phys.* **1986**, *84*, 5606. See also: Ahlrichs, R.; Scharf, P.; Ehrhardt, C. *J. Chem. Phys.* **1985**, *82*, 890.

(13) Frisch, M. J.; Trucks, G. W.; Head-Gordon, M.; Gill, P. M. W.; Wong, M. W.; Foresman, J. B.; Johnson, B. G.; Schlegel, H. B.; Robb, M. A.; Replogle, E. S.; Gomperts, R.; Andres, J. L.; Raghavachari, K.; Binkley, J. S.; González, C.; Martin, R. L.; Fox, D. J.; Defrees, D. J.; Baker, J.; Stewart, J. J. P.; Pople, J. A. GAUSSIAN 92; Gaussian, Inc.: Pittsburgh, PA, 1992.

0002-7863/95/1517-8416$09.00/0

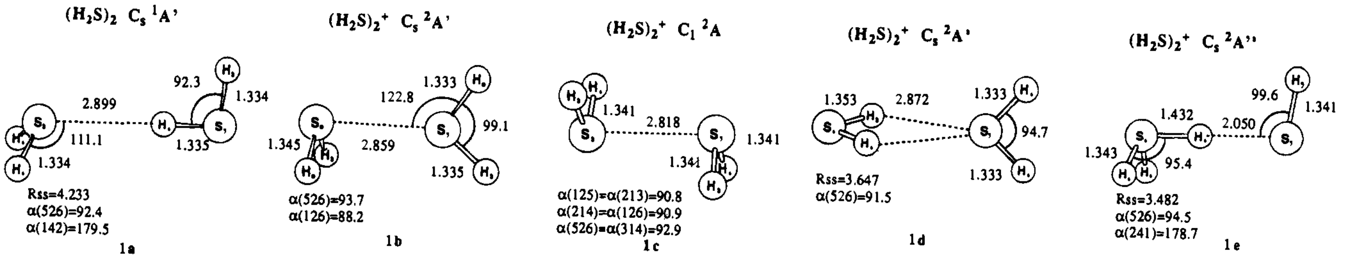

Figure 1. MP2/MC-311G(d,p) optimized geometries for the $(H_2S)_2$ neutral dimer (**1a**) and for the $(H_2S)_2^+$ radical cation (**1b–e**). Distances are in angstroms and angles in degrees. Structures **1b** and **1d** are first-order saddle points. For comparison the geometry of the monomers is as follows: H_2S, R(H–S) = 1.334, ∠HSH = 92.2; H_2S^+, R(H–S) = 1.351, ∠HSH = 93.3; SH, R(H–S) = 1.338; H_3S^+, R(H–S) = 1.347, ∠HSH = 94.9.

method[12] are also carried out at the MP2 geometries. In all these calculations all the valence electrons of H_2S, PH_3, and ClH are correlated.

The basis set used for the geometry optimizations and frequency calculations is of triple-ζ plus polarization quality. This basis set is specified in the Gaussian92[13] program as MC-311(d,p), and for the P, S, ad Cl atoms it corresponds to the MacLean–Chandler (12s9p)/[6s5p][14] with a d polarization function added ($\alpha_P = 0.55$, $\alpha_S = 0.65$, and $\alpha_{Cl} = 0.75$). The H basis set is the 6-311G basis with a p polarization function ($\alpha = 0.75$) added. The single-points MCPF calculations are done using a larger basis set. This basis set is specified in the Gaussian92 program as MC-311++G(2d,2p) and corresponds to MC-311G for P, S, and Cl and 6-311G for H, supplemented with two polarization functions and one set of diffuse valence functions. The two d polarization functions are $\alpha = 1.1$ and 0.275 for P, $\alpha = 1.30$ and 0.325 for S, and $\alpha = 1.50$ and 0.375 for Cl. The diffuse functions are $\alpha = 0.0348$ for P, $\alpha = 0.0405$ for S, and $\alpha = 0.0483$ for Cl. For the hydrogen atom the polarization functions are $\alpha = 1.50$ and 0.375, and the diffuse function is $\alpha = 0.036$.

We have also optimized $(H_2S)_2$ at the MP2 level using the MC-311++G(2d,2p) basis set. The changes on the geometrical parameters are small, the main difference corresponding to the R_{S-S} distance which decreases 0.082 Å compared to the value obtained with the smaller basis set. As a result, the MCPF dissociation energies agree to better than 0.1 kcal/mol regardless of whether the equilibrium geometries are obtained with the MC-311(d,p) or with the MC-311++(2d,2p) basis set. Also, the effect of the geometry changes when increasing the basis set on the vertical ionization energies is very small, since the largest difference is 0.03 eV. Thus, we do not expect significant differences because of using the smaller basis set in the optimization process.

The MP2 calculations were performed using the Gaussian92 program[13] and the open shell calculations were based on a spin-unrestricted SCF treatment. In all these calculations, spin contamination was found to be small. MCPF calculations were carried out using MOLECULE-SWEDEN program systems[15] and were based on a spin-restricted treatment.

Results and Discussion

We will first present and discuss the results obtained in the ionization of each dimer individually and then discuss the general trends.

A. $(H_2S)_2$ and $(H_2S)_2^+$. An experimental study by Dyke et al. shows that the $(H_2S)_2$ dimer can have either a C_s linear hydrogen bonded structure or a C_{2v} bifurcated structure, since both structures are compatible with the electric deflection results.[16] In agreement with previous theoretical studies,[17–19] our calculations, at the MP2/MC-311G(d,p) level of theory, show that the C_s open structure is more stable than the C_{2v} bifurcated one, the latter structure not even being a minimum on the potential energy surface. Thus, we have considered the linear C_s structure to study the ionization process and subsequent rearrangements.

In Figure 1 we present the MP2 optimized geometrical parameters of the neutral $(H_2S)_2$ dimer C_s structure (**1a**) as well as those of the relaxed structures obtained after ionization (**1b–e**). It can be observed that the formation of the hydrogen bond increases the H_4–S_1 distance by only 0.001 Å, which is smaller than the lengthening (0.006 Å) computed for the $(H_2O)_2$ dimer.[2] Moreover, the intermolecular S_2–H_4 distance (2.899 Å) is much larger than that of the water dimer (1.942 Å). This was to be expected considering the already known much weaker hydrogen bonding for the second-row hydride molecules.[20] The computed binding energy of $(H_2S)_2$ at the MCPF level using the MC-311++G(2d,2p) basis set and without including the zero-point correction is 1.4 kcal/mol, in good agreement with experimental results.[21]

Let us now consider the ionization process of the $(H_2S)_2$ dimer. Ionization can occur either in the proton donor molecule or in the proton acceptor one. The first ionic state is a $^2A''$ state that arises from removing the electron from the HOMO orbital, a″, of the dimer, which corresponds to the lone pair $2b_1$ orbital of the proton donor molecule. The second ionic state is the $^2A'$ state derived from ionizing the a′ orbital immediately lower to the HOMO orbital of the dimer, which mainly corresponds to the $2b_1$ orbital of the proton acceptor monomer. This description of the ionic states is consistent with the MCPF atomic charges. That is, while in the $^2A''$ state the positive charge lies on the proton donor monomer (0.95), in the $^2A''$ state it lies on the proton acceptor one (0.99).

The MCPF vertical ionization energies computed using the MP2 equilibrium geometries are 10.27 and 9.81 eV for the $^2A'$ and $^2A''$ states, respectively. These values are in reasonably good agreement with the values determined experimentally of 10.95 and 9.75 eV.[6] As expected, the first vertical ionization potential IP ($^2A''$ state) is smaller than the one computed, at the same level of calculation, for free H_2S (10.12 eV). The decrease of the first vertical IP when compared to that of the free monomer was also observed for the $(H_2O)_2$ dimer,[2] and it is due to the destabilization of the HOMO orbital of the proton donor molecule because of the formation of the hydrogen bond. However, the second vertical IP of the dimer is larger than that of free H_2S because the hydrogen bonding stabilizes the HOMO orbital of the acceptor monomer.

The geometry relaxation of the $^2A'$ state, keeping C_s symmetry in the calculation, leads to structure **1b** displayed in Figure

---

(14) McLean, A. D.; Chandler, G. S. *J. Chem. Phys.* **1980**, *72*, 5639.

(15) MOLECULE-SWEDEN is an electronic structure structure program written by J. Almlöf, C. W. Bauschlicher, M. R. A. Blomberg, D. P. Chong, A. Heiberg, S. R. Langhoff, P.-Å. Malmqvist, A. P. Rendell, B. O. Roos, P. E. M. Siegbahn, and P. R. Taylor.

(16) Odutola, J. A.; Viswanathan, R.; Dyke, T. R. *J. Am. Chem. Soc.* **1979**, *101*, 4787.

(17) Frisch, M. J.; Pople, J. A.; Del Bene, J. E. *J. Phys. Chem.* **1985**, *89* 3664.

(18) Amos, R. D. *Chem. Phys.* **1986**, *104*, 145.

(19) Kerns, R. C.; Allen, L. C. *J. Am. Chem. Soc.* **1978**, *100*, 6587.

(20) Sennikov, P. G. *J. Phys. Chem.* **1994**, *98*, 4973.

(21) Sennikov, P. G.; Raldwgin, G. A.; Sckrunin, V. E.; Tokhadze, K. G. *J. Mol. Struct.* **1990**, *219*, 203.

Table 1. MCPF (MC-311++G(2d,2p)) Relative Energies, with Respect to the Isolated H_2S and H_2S^+ Molecules, for the Vertical Ionized $(H_2S)_2^+$ Dimer in the $^2A'$ ad $^2A''$ States and for Their Derived Radical Cations[a]

structure	state	ΔE (kcal/mol)
$H_2S + H_2S^+$	$^1A_1 + {}^2B_1$	0.0
$[H_2S-HSH]^+$ (**1a**)	2A′	2.1
$[H_2S-HSH]^+$ (**1a**)	2A″	−8.6
$[H_2S-SH_2]^+$ (**1b**)	2A′	−11.7
$[H_2S-SH_2]^+$ (**1c**)	2A	−29.0
$[SH_2-SH_2]^+$ (**1d**)	2A′	−7.7
$[[SH_3^+-SH]$ (**1e**)	2A″	−17.3
$SH_3^+ + SH$	$^1A_1 + {}^2\Pi$	−5.3

[a] Geometries are taken from the MP2 calculations.

1. It should be noted that at the beginning of the optimization process the S−S distance increases significantly. Then, after reorientation of the two monomers the S−S distance starts decreasing and we finally get structure **1b**. This structure is analogous to the one we obtained for $(H_2O)_2^+$ after relaxing the $^2A'$ state,[2] and it corresponds to a three-electron interaction between the $2b_1$ monooccupied orbital of the ionized monomer and the $5a_1$ doubly occupied orbital of the other monomer. Because of this three-electron interaction, the positive charge is now more delocalized on the two monomers, 0.81 on the original acceptor monomer and 0.19 on the other one. Frequency calculations show that this structure is not a minimum but a saddle point. Following the imaginary mode and releasing the symmetry constraints we get structure **1c** depicted in Figure 1. Now the two orbitals involved in the three-electron interaction are the $2b_1$ orbitals of the two monomers and thus the positive charge is completely delocalized (0.5 in each monomer). Because ionizing the proton acceptor monomer increases its acidity we have also optimized the bifurcated structure, **1d**, in which the original acceptor monomer is acting as a proton donor. As was found for the $(H_2O)_2^+$ dimer,[2] such a structure is found to be a saddle point on the potential energy surface.

Geometrical relaxation of the $^2A''$ ionic state leads to the proton-transfer SH_3^+-SH complex depicted in Figure 1e. Frequency calculations show that this structure is a minimum in contrast to the results of Radom et al.,[3] which found it to be a transition state and to spontaneously collapse to the three-electron hemibond structure, **1c**, when the calculation was performed without any symmetry constraints. Although both calculations have been carried out at the same correlated MP2 level, the basis set used in the present work, MC-311G(d,p), is larger than the 6-31G* used by Radom. Thus, our calculations seem to indicate that both the hemibond structure and the proton-transfer complex are minima on the potential energy surface. However, the frequency value corresponding to the symmetry breaking mode in the proton-frequency complex (**1e**) is very small indicating that the surface is very flat.

In Table 1 we present the MCPF relative energies calculated with respect to the isolated $H_2S + H_2S^+$ molecules for all the stationary points depicted in Figure 1. We have also included the relative energies of the two vertical $^2A'$ and $^2A''$ states. As expected, the lowest vertical ionic state, $^2A''$, lies below the $H_2S + H_2S^+$ asymptote, due to the decrease of the vertical IP of the dimer compared to that of free H_2S. However, the $^2A'$ state lies above the dissociation limit, $H_2S + H_2S^+$, because the increase of the second vertical IP of the dimer compared to that of H_2S is larger than the hydrogen bonding energy of the neutral dimer.

The proton-transfer complex SH_3^+-SH (**1e**), which arises from the geometrical relaxation of the $^2A''$ state, is 8.7 kcal/mol (0.38 eV) lower than the vertical ionized $^2A''$ state. Thus, the adiabatic IP corresponding to the $^2A''$ state is 9.43 eV. The difference between the vertical and adiabatic ionization potential (0.38 eV) is larger than that of the monomer H_2S (0.01 eV), due to the larger distortion of the dimer upon ionization. This difference is significantly smaller than the 0.91 eV found for the water dimer.[2] Moreover, in contrast to the water dimer, the proton-transfer complex (**1e**) does not correspond to the global minimum of the potential energy surface. Instead, the three-electron hemibond structure, Figure 1c, derived from the second ionic state $^2A'$, is found to be the most stable isomer. This is in contrast to the SCF results of Raol et al.,[6] which did not get any stable minimum from the relaxation of the $^2A'$ state. Their results appeared to indicate that the ionized dimer dissociated into H_2S and H_2S^+. However, as has already been mentioned, during the relaxation process of the $^2A'$ state, the distance between the two monomers increases significantly before they reorient to evolve to the hemibond complex. Structure **1c** is 31.1 kcal/mol (1.35 eV) lower than the vertical ionized $^2A'$ state and so the adiabatic IP corresponding to this state is 8.92 eV.

Two experimental studies have reported values of 9.74 ± 0.01[22,23] and 9.596 ± 0.002 eV[24] for the adiabatic ionization energy of $(H_2S)_2$. While the computed adiabatic IP corresponding to the $^2A''$ state (9.43 eV) agrees reasonably well with these experimental values, the adiabatic IP of the $^2A'$ state (8.92 eV) is too low to explain the experimental results. Thus, our calculations suggest that the proton-transfer complex is the specie which is observed in the experimental studies. Moreover, in the experimental study of Blais and Walters,[23] the $SH_3^+ + SH$ asymptote is found to be 0.52 eV (11.9 kcal/mol) above the $(H_2S)_2^+$ structure and the dissociation energy of the dimer cation with respect to H_2S and H_2S^+ is estimated to be 0.74 ± 0.01 eV (17.1 ± 0.3 kcal/mol). This again strongly suggests that the observed structure of $(H_2S)_2^+$ corresponds to the proton-transfer complex SH_3^+-SH, since MCPF calculations indicate that it lies 12.0 kcal/mol below the $SH_3^+ + SH$ asymptote and the computed dissociation energy is 17.3 kcal/mol. The three-electron hemibond structure has a dissociation energy of 29.0 kcal/mol, too large compared with the experimental results. A value of 0.92 eV (21.2 kcal/mol) for the dissociation energy of $(H_2S)_2^+$ has also been estimated from another experimental study.[24] This value is somewhat larger than the previous experimental value of 17.1 kcal/mol but it is still closer to the one we have computed for the proton-transfer complex than to that of the hemibonded structure.

In a recent ultraviolet photoelectron spectroscopic study of $(H_2S)_2$, Rao et al.[6] reported a value of 9.56 eV for the adiabatic IP of the $^2A''$ state and a value of 10.75 eV for the adiabatic IP of the excited $^2A'$ state. While the adiabatic IP of the $^2A''$ state agrees well with previous experimental values and with the value computed in the present work, the adiabatic IP of the $^2A'$ state is much larger than our computed value of 8.92 eV. This large difference suggests that the hemibond structure is not observed in the experiments and that dissociation is probably occurring when the dimer is ionized in the $^2A'$ state.

B. (PH_3-H_2S) and $(PH_3-H_2S)^+$. Because H_2S is more acid than PH_3 the most stable hydrogen bonded structure is expected to be that in which the H_2S monomer is acting as the proton donor and the PH_3 monomer as the proton acceptor. In Figure 2 we present the MP2 optimized structures of the neutral PH_3-H_2S dimer and of the different stationary points found after ionization. As in the case of the $(H_2S)_2$ dimer and of the first-row analog H_3N-H_2O,[2] the hydrogen bonding is predicted

---

[22] Walters, E. A.; Blais, N. C. *J. Chem. Phys.* **1981**, *75*, 4208.

[23] Walters, E. A.; Blais, N. C. *J. Chem. Phys.* **1984**, *80*, 3501.

[24] Prest, H. F.; Tzeng, W.-B.; Brom, J. M., Jr.; Ng, C. Y. *J. Am. Chem. Soc.* **1983**, *105*, 7531.

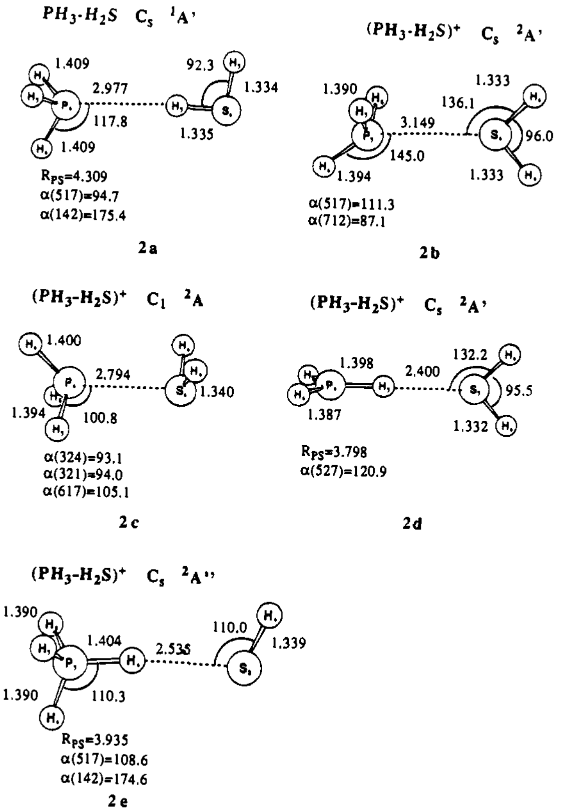

Figure 2. MP2/MC-311G(d,p) optimized geometries for the (PH_3−H_2S) neutral dimer (**2a**) and for the (PH_3−H_2S)$^+$ radical cation (**2b**−**e**). Distances are in angstroms and angles in degrees. Structures **2b** and **2d** are second-order saddle points. For comparison the geometry of the monomers is as follows: PH_3, R(P−H) = 1.410, ∠HPH = 94.2; PH_3^+, R(P−H) = 1.391, ∠HPH = 112.9; PH_4^+, R(P−H) = 1.389.

to be almost linear. As was to be expected, given the much weaker hydrogen bonding interaction for the second-row dimers, the formation of the hydrogen bond increases the H_4−S_2 distance by only 0.001 Å in contrast to the 0.012 Å value calculated for the H_3N−H_2O dimer. Also, the computed MCPF binding energy of PH_3−H_2S (1.3 kcal/mol) is significantly smaller than the value of 6.4 kcal/mol computed for NH_3−H_2O.

The computed ionization potential of PH_3 (9.62 eV) is smaller than the ionization potential of H_2S (10.12 eV). Thus, ionizing PH_3 in the dimer is expected to be more favorable than ionizing H_2S. However, because the hydrogen bonding formation destabilizes the HOMO orbital of the donor monomer (H_2S) and stabilizes the HOMO orbital of the acceptor (PH_3), ionizing H_2S becomes the most favorable process. That is, the lowest ionic state is the $^2A''$ state which arises from removing the electron from the $2b_1$ orbital of H_2S and the second ionic state is the $^2A'$ derived from removing the electron from the $5a_1$ orbital of PH_3. Consistently, the MCPF atomic charges show that in the $^2A''$ state the positive charge is almost entirely on the H_2S monomer (0.92), while in the $^2A'$ state it is almost entirely located on the acceptor monomer (0.98). The MCPF vertical ionization potentials corresponding to the $^2A''$ and $^2A'$ states are 9.78 and 10.42 eV.

The geometry optimization of the vertical ionized $^2A'$ state, keeping C_s symmetry constraints, leads to structure **2b** displayed in Figure 2. As was already observed in the geometry relaxation of the $^2A'$ state of $(H_2S)_2^+$, the distance between the two monomers increases significantly during the optimization process. Then the two monomers reorient and the P−S distance starts decreasing to finally get the three-electron structure **2b**. This hemibond structure mainly arises from the interaction between the $5a_1$ monoccupied orbital of PH_3 and the $5a_1$ doubly occupied orbital of H_2S, and it is analogous to the one we found for the first-row $(H_3N$−$H_2O)^+$ radical cation. However, in contrast to the first-row radical cation,[2] structure **2b** is found to have two imaginary frequencies. Releasing symmetry constraints we obtain structure **2c** for which the three-electron bond is now derived from the interaction between the $5a_1$ orbital of PH_3^+ and the $2b_1$ orbital of H_2S. MCPF atomic charges show that now the positive charge is more delocalized in the two monomers (0.55 on PH_3 and 0.45 on H_2S) than in the ionized $^2A'$ state (0.98 on PH_3 and 0.02 on H_2S) or the previous three-electron structure **2b** (0.91 on PH_3 and 0.09 on H_2S). Thus, delocalization seems to be more favorable when the HOMO orbital of H_2S instead of the $5a_1$ orbital is the one involved in the three-electron interaction. This is due to the fact that the energy difference between the two interacting orbitals is smaller in structure **2c** than in structure **2b**.

Table 2. MCPF (MC-311++G(2d,2p)) Relative Energies, with Respect to the Isolated H_2S and PH_3^+ Molecules, for the Vertical Ionized $(PH_3$−$H_2S)^+$ Dimer in the $^2A'$ and $^2A''$ States and for Their Derived Radical Cations[a]

structure	state	ΔE (kcal/mol)
$PH_3^+ + H_2S$	$^2A_1 + {}^1A_1$	0.0
$PH_3 + H_2S^+$	$^1A_1 + {}^2B_1$	11.6
$[H_3P$−$HSH]^+$ (**2a**)	$^2A'$	17.3
$[H_3P$−$HSH]^+$ (**2a**)	$^2A''$	2.4
$[H_3P$−$SH_2]^+$ (**2b**)	$^2A'$	−7.8
$[H_3P$−$SH_2]^+$ (**2c**)	^2A	−22.6
$[H_2PH$−$SH_2]^+$ (**2d**)	$^2A'$	−3.4
$[PH_4^+$−SH] (**2e**)	$^2A''$	−18.2
PH_4^+ + SH	$^1A_1 + {}^2\Pi$	−11.6

[a] Geometries are taken from the MP2 calculations.

Given that the ionization of PH_3 increases its acidity, we have also optimized a structure with the PH_3^+ monomer acting as the proton donor (see Figure 2d). Such a structure was found to be the most stable one for the first-row $(NH_3$−$H_2O)^+$ radical cation.[2] However, for the $(PH_3$−$H_2S)^+$ structure **2d** is found to have two imaginary frequencies. Geometrical optimization of the $^2A''$ state leads to the proton-transfer PH_4^+−SH complex (see Figure 2e).

In Table 2 we present the MCPF relative energies with respect to the isolated PH_3^+ and H_2S molecules for all the stationary points shown in Figure 2. For comparison the relative energies of the two vertical $^2A'$ and $^2A''$ states have also been included. It can be observed that the most stable structure for the $(PH_3$−$H_2S)^+$ radical cation corresponds to the hemibond structure **2c**, obtained after relaxation of the vertical $^2A'$ state. However, because the vertical $^2A'$ state lies 17.3 kcal/mol above the PH_3^+ + H_2S asymptote, this state could also evolve to the dissociated PH_3^+ + H_2S. In fact, the MP2 optimization seemed to indicate that dissociation needs to occur before the formation of the hemibond complex. Only 4.4 kcal/mol above the global minimum lies the proton-transfer PH_4^+−SH complex, derived from the $^2A''$ state. This proton-transfer complex, **2e**, has a binding energy of 6.6 kcal/mol with respect to the PH_4^+ + SH asymptote. Given that this asymptote lies 14.0 kcal/mol below the vertical $^2A''$ state, the products resulting from ionization of the H_2S monomer of the dimer would either be the proton-transfer PH_4^+−SH complex (**2e**) or the dissociated PH_4^+ + SH molecules.

C. ClH−H_2S and (ClH−H_2S)$^+$. The ClH molecule is more acid than H_2S. Thus, the most stable hydrogen bonded dimer is expected to have ClH acting as the proton donor and H_2S as the proton acceptor. In Figure 3 we present the MP2 optimized structures of the neutral ClH−H_2S dimer and of the different isomers of the (ClH−H_2S)$^+$ radical cation. The equilibrium structure of the neutral dimer has C_s symmetry with

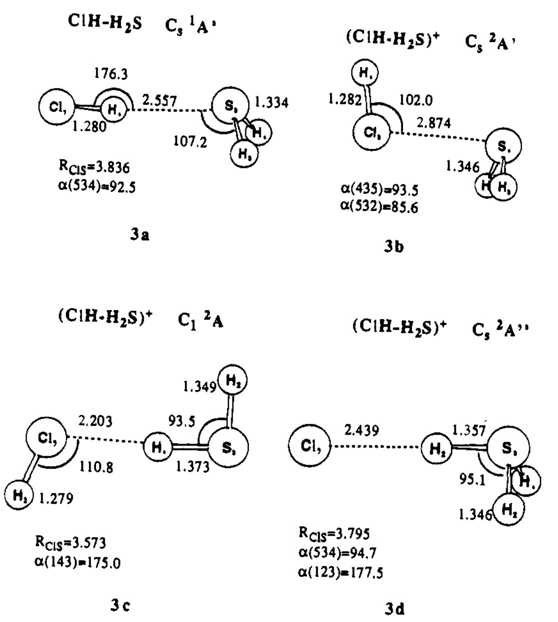

Figure 3. MP2/MC-311G(d,p) optimized geometries for the (ClH−H_2S) neutral dimer (**3a**) and for the $(ClH-H_2S)^+$ radical cation (**3b**−**d**). Distances are in angstroms and angles in degrees. For comparison the geometry of the monomers is as follows: ClH, *R*(Cl−H) = 1.273; ClH^+, *R*(Cl−H) = 1.309.

an almost linear hydrogen bond. The lengthening of the Cl_1−H_2 distance due to hydrogen bonding formation is 0.007 Å. This increase is somewhat larger than the 0.001 Å increase observed for the two previous $(H_2S)_2$ and (PH_3−H_2S) dimers but smaller than the one computed (0.017 Å) for the first-row (FH−H_2O) analog.[2] Also, the intermolecular H_2−S_3 distance is smaller in ClH−H_2S than in $(H_2S)_2$ and PH_3−H_2S. The computed MP2 Cl−S distance is in good agreement with the experimental value of 3.809 Å.[25] The MCPF binding energy is 2.9 kcal/mol, in good agreement with ACPF calculations.[26,27] This value is larger than the binding energy of $(H_2S)_2$ and PH_3−H_2S, but significantly smaller than the one computed for HF−H_2O (8.7 kcal/mol).[2]

The first ionic state is a $^2A'$ state derived by removing the electron from the HOMO orbital of the acceptor (H_2S) monomer. The second ionic state is the $^2A''$ state which results from ionizing the out-of-plane pπ orbital of ClH. This is in contrast to the $(H_2S)_2$ and PH_3−H_2S dimers for which the first vertical ionic state ($^2A''$) corresponds to the ionization of the proton donor molecule. This difference is due to the fact that now the difference between the IP of the two monomers is much larger. That is, the IP of ClH is large enough compared to the IP of H_2S that the ionization of H_2S in the dimer is still the most favorable process, even though it is acting as the proton acceptor. The MCPF vertical ionization potential of the $^2A'$ and $^2A''$ states are 10.56 and 11.86 eV, respectively.

Relaxation of the $^2A'$ state leads to the hemibond structure shown in Figure 3b. Again the MP2 optimization seems to indicate that the dimer dissociates into the ClH and H_2S^+ molecules before it evolves to the hemibond structure. The three-electron bond arises from the interaction of the HOMO orbital of H_2S and the pπ in-plane orbital of ClH. As expected, the positive charge is more delocalized in the two monomers. That is, while in the vertical $^2A'$ state the charges on H_2S and ClH are 0.99 and 0.01, respectively, in the hemibond structure 3b the charges are 0.78 and 0.22. It should be noted that this three-electron hemibond structure (**3b**) was ot found for the first-row $(FH-H_2O)^+$ radical cation.[2] Instead, relaxation of the $^2A'$ state led to a structure in which the FH monomer was acting as the proton acceptor and H_2O^+ as a proton donor. Thus, a similar structure has been optimized for the $(ClH-H_2S)^+$ radical cation (see Figure 3c). This structure is a minimum on the potential energy surface but, as will be shown later, is less stable than the hemibond complex **3b**. Figure 3d shows the proton-transfer $Cl-SH_3^+$ complex obtained after relaxation of the $^2A''$ state.

Table 3. MCPF (MC-311++G(2d,2p)) Relative Energies, with Respect to the Isolated ClH and H_2S^+ Molecules, for the Vertical Ionized $(ClH-H_2S)^+$ Dimer in the $^2A'$ and $^2A''$ States and for Their Derived Radical Cations[a]

structure	state	Δ*E* (kcal/mol)
ClH + H_2S^+	$^1\Sigma^+ + {}^2B_1$	0.0
ClH^+ + H_2S	$^2\Sigma + {}^1A_1$	53.4
$[ClH-SH_2]^+$ (**3a**)	$^2A'$	7.2
$[ClH-SH_2]^+$ (**3a**)	$^2A''$	37.2
$[HCl-SH_2]^+$ (**3b**)	$^2A'$	−11.3
$[HCl-HSH]^+$ (**3c**)	^2A	−7.9
$[Cl-SH_3^+]$ (**3d**)	$^2A''$	0.2
Cl + SH_3^+	$^2P + {}^1A_1$	5.1

[a] Geometries are taken from the MP2 calculations.

Table 4. MCPF Vertical IP_v and Adiabatic IP_{ad} Ionization Energies (eV)[a,b]

			IP_v		IP_{ad}		
	IP_{ad}		$^2A'$	$^2A''$	hb[c]	npt[d]	pt[e]
NH_3	9.93	NH_3-H_2O	11.20	11.10	9.44	9.18	9.22
H_2O	12.32	H_2O-H_2O	12.91	11.46	10.98		10.55
FH	15.77	H_2O-HF	13.54	14.35		11.75	12.10
PH_3	9.62	PH_3-H_2S	10.42	9.78	8.69		8.89
H_2S	10.12	H_2S-H_2S	10.27	9.81	8.92		9.43
ClH	12.43	H_2S-HCl	10.56	11.86	9.76	9.90	10.25

[a] Geometries are taken from the MP2 calculations. [b] First-row results taken from ref 2. [c] Three-electron hemibond structures. [d] Non-proton-transfer complexes. [e] Proton-transfer complexes.

The MCPF relative energies, with respect to the isolated H_2S^+ and ClH molecules, of all the stationary points found after ionization as well as those of the vertical $^2A'$ and $^2A''$ states are given in Table 3. The two vertical $^2A'$ and $^2A''$ states lie within the two asymptotes ClH + H_2S^+ and ClH^+ + H_2S, the $^2A'$ state being the most stable. It can be observed that the most stable isomer of the $(ClH-H_2S)^+$ radical cation corresponds to the hemibond structure **3b**, derived from the $^2A'$ state. Structure **3c** which has H_2S^+ acting as the proton donor is found to be 3.4 kcal/mol less stable than the hemibond structure. This is in contrast to $(HF-H_2O)^+$ for which this structure was found to be the most stable.[2] The proton-transfer complex $Cl-H_3S^+$, structure **3d**, lies significantly higher than the global minimum. Thus, the products resulting from ionization would either be the hemibond $(HCl-H_2S)^+$ complex and the dissociated ClH + H_2S^+ molecules or the proton-transfer $Cl-H_3S^+$ and the dissociated ClH + H_2S^+ molecules or the proton-transfer Cl−H_3S^+ and the dissociated Cl + H_3S^+ fragments, depending on which monomer has been ionized.

D. Trends. In order to discuss the trends in the ionization process of these hydrogen bonded complexes and to contrast them with the first-row analogs we present in Table 4 the MCPF vertical and adiabatic ionization potentials of the first- and second-row dimers. For comparison we have also included the adiabatic IP of all the monomers. For all the considered dimers the two lowest ionic states are the $^2A'$ and $^2A''$ states, depending on whether the ionization is produced in the proton acceptor or in the proton donor monomer, respectively. The hydrogen

---

(25) Legon, A. C.; Millen, J. D. *Proc. R. Soc. A* **1988**, *417*, 21.

(26) Bacskay, G. B.; Kerdraon, D. I.; Hush, N. S. *Chem. Phys.* **1990**, *144*, 53.

(27) Bacskay, G. B.; *Mol. Phys.* **1992**, *77*, 61.

bonding formation increases/decreases the energy required to ionize the acceptor/donor monomer. Thus, for the symmetrical dimers and for those dimers formed by two monomers of similar IP, NH_3-H_2O and PH_3-H_2S, the most stable ionic state is the $^2A''$ state. However, for the $FH-H_2O$ and $ClH-H_2S$ dimers, the IP of the proton donor molecule is large enough compared to that of the proton acceptor one that the $^2A'$ state is the lowest one.

In all cases the $^2A''$ state evolves to a proton-transfer complex (pt) due to the increase of acidity of the donor monomer when it is ionized. This proton-transfer complex is the most stable isomer for the $(H_2O)_2$ dimer only. For the other systems, the global minimum is derived from the $^2A'$ state. This global minimum can be either the three-electron hemibond complex (hb) or the non-proton-transfer complex (npt) in which the original acceptor monomer is acting as the proton donor.

For the first-row dimers, excluding $(H_2O)_2$, the non-proton-transfer complex is the most stable, the hemibond complex not even being found for the $(HF-H_2O)^+$ radical cation. However, for the second-row dimers the three-electron hemibond complex is always the most stable structure. This is due to the different stability between the hemibond complexes and the non-proton-transfer complexes in the first and second row. It has already been pointed out that the stability of three-electron bond complexes decreases as the difference between the IP of the two interacting monomers increases.[7,10] Thus, excluding the symmetrical $(H_2O)_2^+$ and $(H_2S)_2^+$, for which $\Delta IP = 0$, it is not surprising that the hemibond complexes are more stable for the second-row dimer cations than for the first-row cations since the difference between the IP of the monomers is much smaller in the second-row hydrides. In fact, no hemibond complex was found for $(FH-H_2O)^+$ probably because the IP of FH is much larger than that of H_2O. For the same reason the non-proton-transfer complex with H_2O^+ acting as donor is more stable than the proton-transfer $F-H_3O^+$ complex. The fact that the hemibond structures of the second row become significantly more stable than the proton-transfer complexes compared to the first-row structures is due not only to the larger stabilization of these compounds, because of a smaller ΔIP, but also to the fact that the proton-transfer complexes are less stable for the second-row systems. That is, proton-transfer reactions are more favorable between first-row monomers mainly because the bond dissociation energy, H^+-AH_{n-1}, of the ionized proton donor is larger in the second-row molecules. The differences between the proton affinities of the first- and second-row monomers does not seem to be the determinant factor. Note that while the proton affinity of NH_3 is somewhat larger than that of PH_3 the proton affinities of H_2S and H_2O are very similar. Also, electrostatic interactions in the proton-transfer complex $BH_{n+1}{}^+-AH_{n-1}$ are more important in the first-row systems due to the smaller intermolecular distances.

In summary, several factors such as the difference between the IP of the monomers, its variation because of hydrogen bonding formation, and the exothermicity of the proton-transfer reactions between the donor and the acceptor monomers should be taken into account to understand the relative energies of the two vertical ionic states and those of the relaxed structures.

Conclusions

The vertical ionization potentials of H_2S-H_2S, PH_3-H_2S, and $FH-H_2S$ hydrogen bonded dimers and its subsequent rearrangement processes have been studied using large basis sets and including correlation energy at the MCPF level. Optimizations were performed at the MP2 level of calculation. The two lowest states arise from ionizing the proton donor monomer or the proton acceptor molecule. In the first case, the dimer evolves to a proton-transfer complex. In the second case the dimer seems to dissociate before it rearranges to form a three-electron hemibond complex. This hemibond complex has been shown to be the global minimum on the potential energy surface in contrast to the first-row dimers. However, the comparison of our results with the experimental ones for $(H_2S)_2$ seems to indicate that the observed specie in the experiments is the proton-transfer complex and not the most stable hemibond structure. This is due to the fact that ionization in the first ionic state leads to the proton-transfer isomer, while ionization to the second state cause the dissociation of the dimer. Thus, the way in which the hemibond complex is obtained in the experiments becomes an experimental challenge.

Acknowledgment. We thank the Catalonia Supercomputing Center (CESCA) and the Center for Parallelism of Barcelona (CEPBA) for providing time on the CRAY Y-MP and Convex C-3480 computers, respectively. We would also like to thank Charles W. Bauschlicher for providing a copy of the SWEDEN-MOLECULE system programs. Financial support from DGI-CYT through project PB89-0318 is also gratefully acknowledged.

JA9504909